

# Mechanistic pathways of aromatic nucleophilic substitution in conventional solvents and ionic liquids†

Cite this: *New J. Chem.*, 2014, **38**, 2611

Marcela Gazitúa,<sup>\*a</sup> Ricardo A. Tapia,<sup>b</sup> Renato Contreras<sup>c</sup> and Paola R. Campodónico<sup>a</sup>

Received (in Porto Alegre, Brazil)  
24th January 2014,  
Accepted 12th March 2014

DOI: 10.1039/c4nj00130c

www.rsc.org/njc

Solvation effects on the reaction mechanism of the title reactions have been kinetically evaluated in 21 conventional solvents and 17 ionic liquids. Solvent polarity affects the catalyzed and non-catalyzed  $S_NAr$  pathways differently. The amphiphilic character of water and formamide, which act as a hydrogen bond donor/acceptor, induces nucleophilic activation at the nitrogen center of the nucleophile. The ionic liquid EMIMDCN appears to be the best solvent for the  $S_NAr$  route probably due to the high polarizability of the dicyanamide anion.

## Introduction

Nucleophilic substitution is an addition–elimination process that depending on the nature of the substrate, the attacking nucleophile and the solvent effect may lead to a nucleophilic substitution ( $S_N$ ) product, a nucleophilic aromatic substitution ( $S_NAr$ ) product, or both.<sup>1</sup> Scheme 1 summarizes the possible routes towards any of both reaction products. When the reaction center is a heteroatom (the left branch in Scheme 1) the reaction mechanism is  $S_N$  and it depends on the stability of the pentavalent intermediate ( $P^\pm$  in Scheme 1) formed. If  $P^\pm$  is not stabilized under the reaction conditions, the process is concerted.<sup>2</sup> Conversely, if  $P^\pm$  is stabilized, a stepwise pathway may be operative.<sup>1</sup> Furthermore, if the nucleophilic attack occurs at the aromatic ring (the right branch in Scheme 1), the reaction is classified as  $S_NAr$ .<sup>1,3–8</sup> This reaction proceeds *via* a stepwise mechanism<sup>1,3–6</sup> that involves: (i) a nucleophilic attack with re-hybridization of the ipso carbon atom on the aromatic ring from  $sp^2$  to  $sp^3$  to form a Meisenheimer complex<sup>1,7,8</sup> (MC1 in Scheme 1) and (ii) the leaving group (LG) departure in a second step to regenerate the  $sp^2$  center through catalyzed or non-catalyzed pathways<sup>1,4–8</sup> ( $k_3$  or  $k_2$ , respectively in Scheme 1).

Solvent effects on  $S_NAr$  reactions have previously been studied in conventional organic solvents (COS)<sup>4,8–11</sup> and more recently in room temperature ionic liquids (RTILs).<sup>12–16</sup> The main focus in these studies was put on the bulk and specific solute–solvent interactions that determine selectivity, reaction rates and mechanisms in these systems. Nudelman *et al.*<sup>9</sup> studied leaving group abilities in the  $S_NAr$  reactions of halo-benzenes towards amines in aprotic COS. These authors found that the rate-limiting step of the reaction mechanism changes when the reaction proceeds in solvents that exhibit hydrogen-bond basicity (HBB) properties. Wang *et al.*<sup>10</sup> reported that HBB of solvents significantly affects the regiochemistry of the  $S_NAr$  reaction between polyfluoroarene derivatives and amines. Park *et al.*<sup>11</sup> investigated the mechanism of  $S_NAr$  of fluorination reactions under the influence of protic solvents and charged nucleophiles. They found that counterions or protic solvents alone retard the  $S_NAr$  reactions, while together they promote the enhancement of reactivity. For these systems, the protic solvent may affect the reaction acting over the counterion as a Lewis base and the nucleophile acting as an ion pair. The presence of charges, as a separated cation–anion pair or as ion pairs, strongly suggests that these results may be used to study solvent effects on chemical reactivity (reaction rates in the present case) in RTILs. D'Anna *et al.*<sup>14</sup> recently reported on the reaction of thiophene derivatives with N-nucleophiles in RTILs. They proposed that the intramolecular interactions at the transition state structure are strongly affected by the reaction medium, determining the selectivity and catalysis of the process.

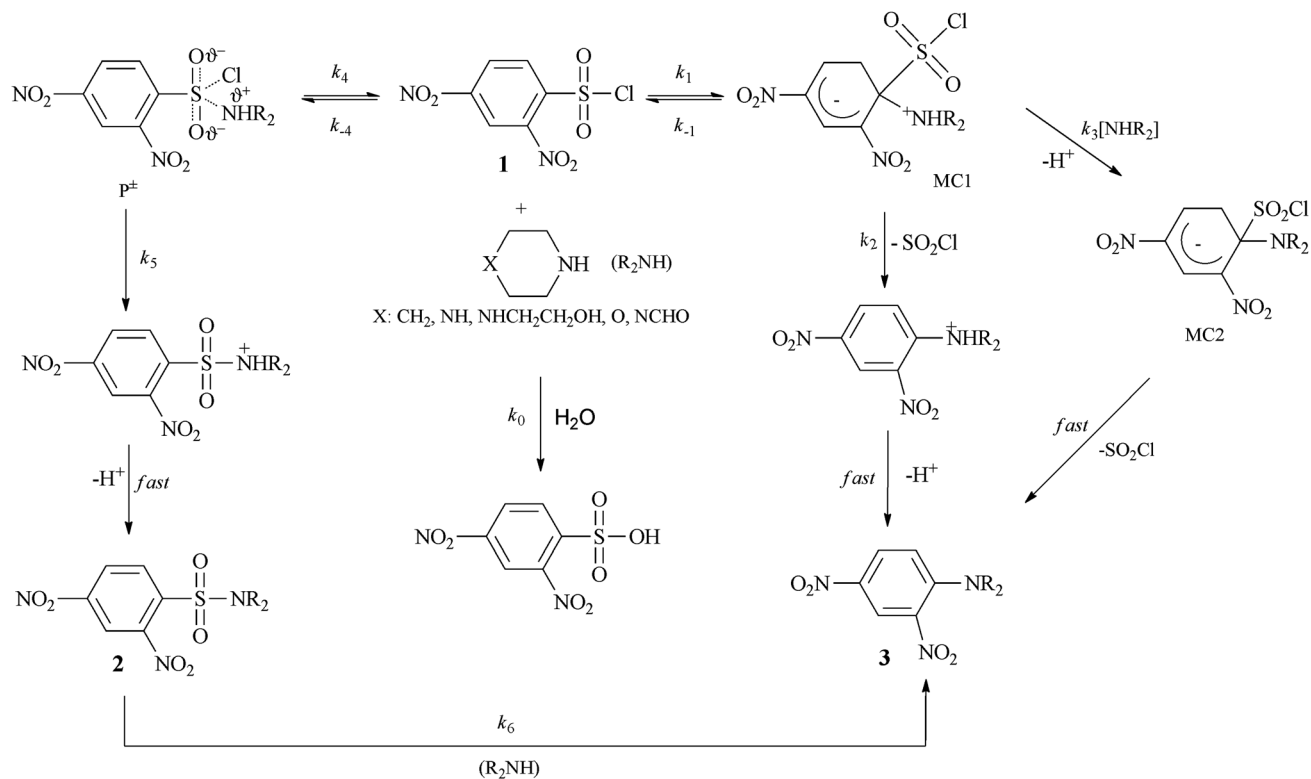
This background prompted us to perform a comparative study of solvation effects in COS and a series of RTILs. However, some preliminary considerations are worth stressing. First of all, the physical interpretation of solvent effects in RTILs is an

<sup>a</sup> Centro de Química Médica, Facultad de Medicina, Clínica Alemana Universidad del Desarrollo, Código Postal 7710162, Santiago, Chile. E-mail: migazitu@uc.cl, pcampodonico@udd.cl; Fax: +56 2 23279639; Tel: +56 2 23279682

<sup>b</sup> Facultad de Química, Pontificia Universidad Católica de Chile, Código Postal 7820436, Santiago, Chile. E-mail: rtapia@uc.cl; Tel: +56 2 23544429

<sup>c</sup> Departamento de Química, Facultad de Ciencias, Universidad de Chile, Casilla 653, Santiago, Chile. E-mail: rcontrer@uchile.cl; Tel: +56 2 29787272

† Electronic supplementary information (ESI) available: Copies of <sup>1</sup>H NMR spectra, rate constant values and experimental conditions. See DOI: 10.1039/c4nj00130c

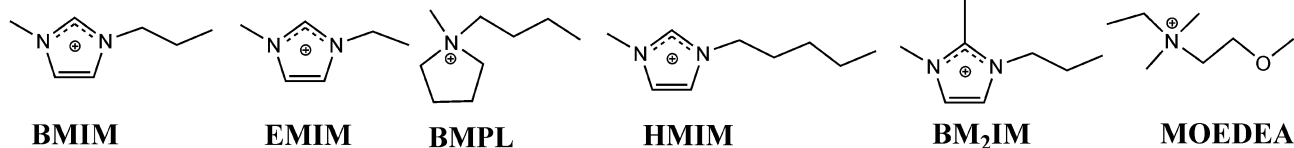


Scheme 1 Possible nucleophilic substitution reactions of DNBSOCl with secondary alicyclic amines.

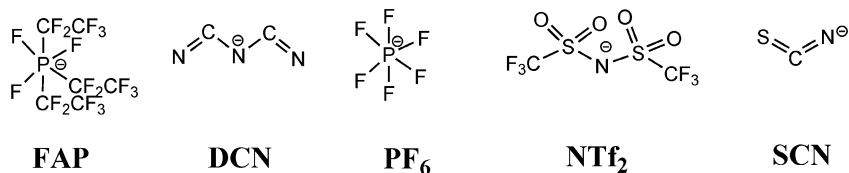
extremely complex problem, because in general, good RTILs (as reaction media) are those species where the anion and cation are associated to a very low extent.<sup>17</sup> This result implies that the target solute–solvent interactions will in general be masked by the leading solvent–solvent interactions that are coulombic in nature. A usual experimental model to rationalize solvation effects on reaction rates in RTIL media is to consider

a reasonably large number of RTILs (17 in the present case) and evaluate their performance as reaction media by fixing the anion and varying the cation and *vice versa*. The criteria for selecting the series of RTILs were based on: (i) the solubility of substrates and nucleophiles; (ii) to have a reasonable number of anions and cations to assess anion and cation effects and to ensure that these RTILs do not interfere with the reaction

### Cations:



### Anions:



### EAN

Scheme 2 Structures and acronyms of the RTILs used in this study.

under study. Scheme 2 shows structures and acronyms of the RTILs used in this study.

## Results and discussion

In this work we use the reaction of 2,4-dinitrophenylsulfonyl chloride (DNBSCl) with secondary alicyclic (SA) amines in aqueous media as a model system to analyze the effect of solvent polarity on the reaction mechanism. We started with the synthesis of 1-(2,4-dinitrophenylsulfonyl)piperidine and 1-(2,4-dinitrophenyl)piperazine (compounds 2 and 3 in Scheme 1), corresponding to the  $S_N$  and  $S_NAr$  reaction products, respectively (synthetic details are given in the Experimental section). The product analysis in water and in acetonitrile (MeCN) shows that 3 is the unique product at the end of the reaction, thereby suggesting an  $S_NAr$  pathway. HPLC analyses were performed to compare the retention times and UV-visible spectra with those of authentic samples in water and in MeCN as reaction media at the end of the reaction (see Fig. S1–S9 in ESI†). However HPLC analyses at different times show that the  $S_N$  product is formed in minor proportion and decomposed in excess of amine to give the  $S_NAr$  product in both cases (see Fig. S8 and S9 in ESI†).

The formation of a unique  $S_NAr$  product discards the possibility of nucleophilic attack at the unsubstituted position on the ring.<sup>18</sup>

Under amine excess, the pseudo first order rate constant ( $k_{obs}$ ) was found for all the reactions. The values of  $k_{obs}$  for all the reactions are in accordance with eqn (1) where  $k_0$  and  $k_N$  are the rate coefficients for solvolysis and aminolysis of the substrate, respectively. These values were obtained as the intercept ( $k_0$ ) and slope ( $k_N$ ) of linear plots of eqn (1) for the reactions of DNBSCl with all amines in water, some COS and all RTILs.

$$k_{obs} = k_0 + k_N[N] \quad (1)$$

In water, for all amines studied, a linear plot of  $k_{obs}$  vs. free amine concentration ( $[N_F]$ ) is observed. These plots pass through the origin, thereby suggesting that the contribution of hydroxide and/or water (*i.e.*, the  $k_0$  step in Scheme 1) to the pseudo first order rate constant ( $k_{obs}$ ) values is negligible<sup>8</sup> and the reactions occurs *via* a non-catalyzed route ( $k_2$  in Scheme 1). Kinetic details are shown in the Experimental section and ESI† (Fig. S10–S15 and Tables S1–S15).

Previous reports suggest that this kind of reactions proceed through a rate-limiting formation of MC1.<sup>8,19</sup> However, the statistically corrected Brønsted-type plot for the reference solvent (water) is linear with  $\beta_{nuc} = 0.8$  a value close to that observed in the ester aminolysis, where the LG departure is rate determining.<sup>20</sup> It seems then that the bond formation between the nucleophiles and the substrate is fully advanced in the rate-limiting transition state. Table 1 shows the nucleophilic rate constants and  $pK_a$  values in water needed to build up the Brønsted type-plot. Note that piperidine is a basic amine that tends to deprotonate more easily which is in agreement with  $k_N$  values found for SA amines.

In order to examine the solvent effects on the reaction mechanism, we studied the reaction between DNBSCl and piperidine in a series of 20 COS and 17 RTILs using the reaction

**Table 1**  $pK_a$  and  $k_N$  values for the reactions of SA amines with DNBSCl in water<sup>a</sup>

Amine	$pK_a$ <sup>21</sup>	$10^4 k_N/s^{-1} M^{-1}$
Piperidine	11.24	306.4 ± 4.8
Piperazine	9.94	51.9 ± 0.78
1-(2-Hydroxyethyl)piperazine	9.39	16.1 ± 0.22
Morpholine	8.78	4.95 ± 0.14
1-Formylpiperazine	7.68	0.786 ± 0.04

<sup>a</sup> The value accompanying the  $k_N$  values correspond to error of the slope of a plot of  $k_{obs}$  vs. free amine concentration required to build up Brønsted plots.

in water as a reference. For all reaction media, the final product was confirmed to be compound 3, thereby ratifying an  $S_NAr$  pathway.

Linear plots of  $k_{obs}$  vs.  $[N_T]$  (total amine concentration) for a series of COS and the whole series of RTILs series are coincident with the same kinetic responses found in aqueous media (see Fig. S16–S41 and Tables S16–S42 in ESI†). However, some COS show upward curvature as a function of increasing amine concentration. Such curvature is typical for reactions that proceed through a rate limiting proton transfer (RLPT) mechanism<sup>22</sup> (MC2, right side branch in Scheme 1). Details are given in Fig. S42–S67 and Tables S43–S55 in ESI†. According to Scheme 1, the reaction proceeds through two intermediates (MC1 and MC2) corresponding to a zwitterionic adduct and its deprotonated form, respectively. Table 2 shows the microconstants  $Kk_2$  and  $Kk_3$  for the reaction of DNBSCl with piperidine for a series of COS studied that proceeds through catalyzed pathways. The low contribution of  $Kk_2$  (to promote the LG departure) and  $Kk_3$  (to promote the stabilization of MC2) shows that solvents effects are small in these cases. This result may be traced to the presence of a second molecule of amine that could establish a more favoring interaction to the MC1 compared to that of the solvent molecules. However, solvent polarity may become relevant in the non-catalyzed route.

The “polarity of the solvent” is a rather ambiguous concept, because it encompasses a series of different effects, namely, the static polarizability (dielectric effects) of the solvent; (electronic) polarization of the solvent and specific solute–solvent interactions

**Table 2** Observed microconstants  $Kk_2$  and  $Kk_3$  for the reaction of DNBSCl with piperidine in a series of catalyzed processes in COS<sup>a</sup>

Solvent	$10^3 Kk_2/s^{-1} M^{-1}$	$10^1 Kk_3/s^{-1}$
MeCN	7.25 ± 0.347	0.780 ± 0.0223
THF	0.372 ± 0.0600	0.211 ± 0.00350
CH <sub>2</sub> Cl <sub>2</sub>	1.31 ± 0.317	0.640 ± 0.0204
CHCl <sub>3</sub>	0.500 ± 0.116	0.120 ± 0.00620
C <sub>6</sub> H <sub>6</sub>	1.86 ± 0.314	0.500 ± 0.0170
DMF	8.75 ± 0.191	0.270 ± 0.0106
1,4-Dioxane	0.403 ± 0.109	0.163 ± 0.00820
Acetone	1.53 ± 0.254	0.452 ± 0.0190
Cyclohexane	1.94 ± 0.295	0.85 ± 0.0356
Diethyl ether	1.76 ± 0.420	0.320 ± 0.0320
Ethyl acetate	1.14 ± 0.210	0.300 ± 0.0136
<i>n</i> -Hexane	0.0454 ± 0.431	0.791 ± 0.0402
<i>n</i> -Heptane	0.0328 ± 0.452	1.04 ± 0.0563

<sup>a</sup> The value accompanying the  $Kk_2$  and  $Kk_3$  values correspond to the error of the slope (for  $Kk_2$ ) and the intercept (for  $Kk_3$ ).

**Table 3** Values of  $k_N$  for the reactions of DNBSCl with piperidine in a series of non-catalyzed processes in COS and their Kamlet–Taft parameters

Solvent	$10^4 k_N/s^{-1} M^{-1}$	$\alpha^{2,3}$	$\beta^{2,3}$	$\pi^*^{2,3}$
DMSO	$278 \pm 9$	0.0	0.76	1.0
Ethanol	$7.2 \pm 0.30$	0.86	0.84	0.48
FMA	$547 \pm 11$	0.71	0.48	0.97
H <sub>2</sub> O	$156 \pm 2.2$	1.17	0.18	1.09
<i>tert</i> -Butanol	$16.4 \pm 0.90$	0.68	0.93	0.41
2-Propanol	$6.4 \pm 0.29$	0.76	0.84	0.48
Butanol	$9.2 \pm 0.43$	0.84	0.84	0.47
Methanol	$4.8 \pm 0.12$	0.98	0.66	0.60

$k_N$  values were obtained from the slope of a plot of  $k_{obs}$  vs. total amine concentration.

(typically, hydrogen bonding effects). Kamlet–Taft's linear solvation energy relationship (LSER)<sup>23–26</sup> model does the job in the sense that solvent effects on rate constants may be described by the Hydrogen Bond Acidity (HBA) parameter  $\alpha$ ; the HBB parameter  $\beta$  and the  $\pi^*$  parameter<sup>21</sup> (see Table 3).

Fig. 1(A) shows the relationships between  $\log k_N$  for the non-catalyzed reactions and the  $\alpha$  parameter<sup>23</sup> which is associated with the HBA ability of solvents. In Fig. 1(A) we have two regions independent of their  $\alpha$  values. In the first one, we found dimethylsulfoxide (DMSO), formamide (FMA) and H<sub>2</sub>O grouped as being the best solvents in terms of rate coefficients. On the other hand, we found a second group including all alcohols used in this study. Here there are two points worth mentioning; one is that DMSO, H<sub>2</sub>O and FMA are more polar than alcohols and secondly that they display different hydrogen-bond (HB) accepting/donating abilities. For instance, DMSO presents only HB accepting properties, while H<sub>2</sub>O and FMA can accept and donate HBs. The high rate value for H<sub>2</sub>O suggests the presence of a HB between a hydrogen atom of H<sub>2</sub>O acting as a bridge between the nucleophile and the leaving group at the MC1 structure. This bridge facilitates the relay of electron density from the amine towards the electrophilic centre, thereby enhancing the nucleophilicity of the amine (see Fig. 2).<sup>5</sup>

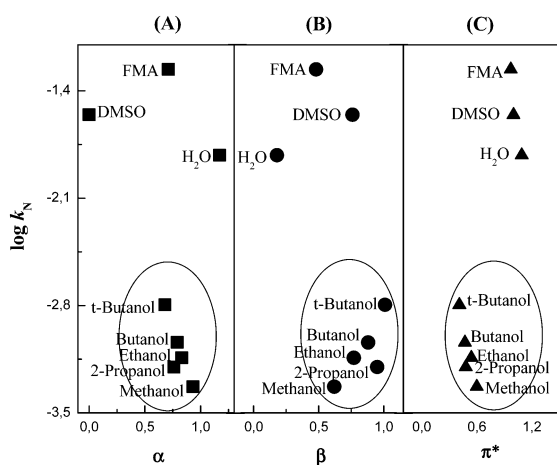


**Fig. 1** Plots of  $\log k_N$  and  $\alpha$  (A),  $\beta$  (B) and  $\pi^*$  (C) for the reactions of DNBSCl with piperidine in a series of non-catalyzed processes in COS.

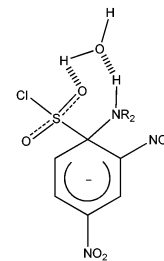


**Fig. 2** General scheme for the possible interaction between H<sub>2</sub>O and the MC1 intermediate.

We further performed the kinetic analysis of the reaction in a 50% w/w ethanol/water mixture and a 90% w/w ethanol/water mixture under the same experimental conditions (see Table S43 in ESI<sup>†</sup>), in order to compare the role of HB effects in these mixtures with water. The rate coefficient H<sub>2</sub>O vs. 50/50 ethanol/water mixture ratio is 5 times slower while that of H<sub>2</sub>O vs. 90/10 ethanol/water mixture is 9 times slower. This result suggests that there may be an increase in reactivity induced by “preferential solvation” in favor of the aqueous phase.<sup>4</sup> Probably, FMA can also form effective HBs with the nucleophile and the leaving group of the MC1 structure. These properties of FMA and H<sub>2</sub>O should account for the high  $k_N$  values observed.

Note that all alcohols have high values of  $\alpha$  parameters, but low  $k_N$  values. This can be traced to its low polarity compared to that of DMSO, FMA and H<sub>2</sub>O.

Fig. 1(B) shows the relationship between  $\log k_N$  and the  $\beta$  parameter,<sup>23</sup> which is a measure of the HBB ability of solvents. Fig. 1(B) displays the same separation between solvents of varying polarity. Here again we have two regions independent of their  $\beta$  values that are worth analyzing. In the first one we found solvents with HB accepting (DMSO) and HB accepting/donating (FMA and H<sub>2</sub>O) abilities that can interact with the proton of piperidine, thereby increasing the electron density on the nitrogen atom.<sup>25</sup> Note that alcohols appear grouped with the same pattern as that shown in Fig. 1(A).

Fig. 1(C) shows the relationships between  $\log k_N$  and  $\pi^*$  parameter<sup>23</sup> which measures the ability of solvents to stabilize a neighboring charge or a dipole by virtue of nonspecific dielectric interactions. Note that the trend is similar to that found for  $\alpha$  and  $\beta$  values shown in Fig. 1(A) and (B). In this figure we have two regions differing in solvent polarity and independent of their  $\pi^*$  values. Since H<sub>2</sub>O, FMA and DMSO have the highest  $\pi^*$  values among all the solvents investigated these reaction media enhance the reaction.

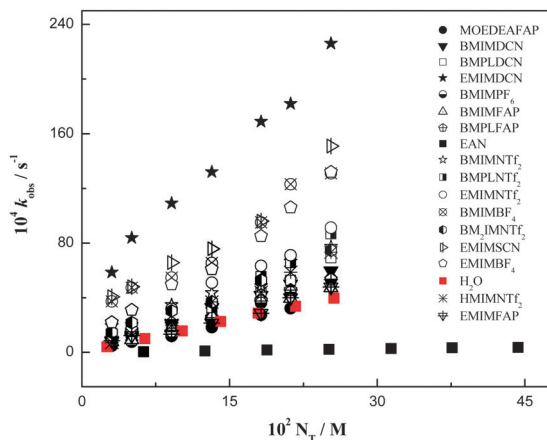
Table 4 shows  $k_N$  values for the reactions of DNBSCl with piperidine in RTILs and their Kamlet–Taft parameters.

Fig. 3 displays linear relationships between  $k_{obs}$  and  $[N_T]$  for the same reaction in the series of 17 RTILs. The comparisons will be made taking water as a reference. We can identify the following classification of the ionic solvents: (i) best solvent: EMIMDCN, (ii) good solvents: BMIMBF<sub>4</sub>, EMIMSCN, EMIMBF<sub>4</sub>, BMIMNTf<sub>2</sub>, BM<sub>2</sub>IMNTf<sub>2</sub>, HMIMNTf<sub>2</sub>, BMPLNTf<sub>2</sub>, EMIMNTf<sub>2</sub>, BMIMFAP, BMPLFAP, BMIMPF<sub>6</sub>, BMIMDCN and BMPLDCN, (iii) similar to water: MOEDEAFAP and EMIMFAP and (iv) very poor solvent: EAN.

**Table 4** Values of  $k_N$  for the reactions of DNBSCl with piperidine in RTILs and their Kamlet–Taft parameters

RTILs	$10^4 k_N/s^{-1} M^{-1}$	$\alpha$	$\beta$	$\pi^*$
EAN	$8.70 \pm 0.35$	$0.85^{27}$	$0.46^{27}$	$1.24^{27}$
BMIMPF <sub>6</sub>	$207 \pm 10.0$	$0.65^{28}$	$0.25^{28}$	$1.02^{28}$
EMIMSCN	$480 \pm 50.0$	nd	nd	nd
BMIMBF <sub>4</sub>	$448 \pm 42.0$	$0.63^{28}$	$0.39^{28}$	$1.04^{28}$
EMIMBF <sub>4</sub>	$489 \pm 28.0$	nd	nd	nd
MOEDEAFAP	$152 \pm 6.30$	nd	nd	nd
EMIMFAP	$179 \pm 17.0$	nd	nd	nd
BMIMFAP	$186 \pm 5.60$	nd	nd	nd
BMPLFAP	$194 \pm 10.0$	nd	nd	nd
BMIMDCN	$235 \pm 5.30$	$0.54^{28}$	$0.60^{28}$	$1.05^{28}$
BMPLDCN	$299 \pm 17.0$	nd	nd	nd
EMIMDCN	$717 \pm 32.0$	$0.54^{27}$	$0.64^{27}$	$1.07^{27}$
BMIMNTF <sub>2</sub>	$266 \pm 21.3$	$0.72^{28}$	$0.24^{28}$	$0.90^{28}$
EMIMNTF <sub>2</sub>	$360 \pm 19.0$	$0.71^{28}$	$0.23^{28}$	$0.98^{28}$
BMPLNTF <sub>2</sub>	$330 \pm 28.0$	$0.57^{28}$	$0.23^{28}$	$0.87^{28}$
BM <sub>2</sub> IMNTF <sub>2</sub>	$263 \pm 15.0$	$0.38^{28}$	$0.26^{28}$	$1.02^{28}$
HMIMNTF <sub>2</sub>	$291 \pm 20.0$	$0.65^{28}$	$0.26^{28}$	$0.97^{28}$

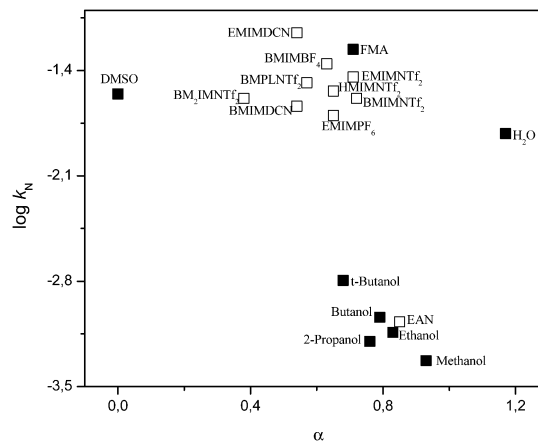
nd: no data available in the literature.  $k_N$  values were obtained from the slope of a plot of  $k_{\text{obs}}$  vs. total amine concentration.

**Fig. 3** Plot of  $k_{\text{obs}}$  against total amine concentration  $[N_T]$  of piperidine for the reactions of DNBSCl with piperidine in a series of RTILs with H<sub>2</sub>O as a reference (red squares).

EAN is the only protic solvent that decreases the reaction rate 17 times vs. H<sub>2</sub>O and 82 times vs. EMIMDCN. EMIMDCN behaves as the best solvent within the series of 38 reaction media analyzed in this work, it presents catalytic behavior at room temperature and therefore it qualifies as the best solvent for this S<sub>N</sub>Ar reaction. Note that EMIMDCN exerts its catalytic property for the pathway that does not involve a second nucleophilic molecule as a catalyst. The pK<sub>a</sub> value of dicyanamide is less than 1.<sup>29</sup> As a result, the nucleophilicity on the nitrogen of piperidine is enhanced. The MC1 forming step is expected to be fast and the leaving group departure becomes rate determining.

If we compare the  $k_N$  values of Table 3 for COS and Table 4 for RTILs we can see that for this S<sub>N</sub>Ar reactions RTILs perform relatively well in comparison with COS.

The analysis of solvent polarity using Kamlet–Taft's linear solvation energy relationship (LSER)<sup>23–26</sup> shows that the comparison of COS vs. RTILs presents the problem that for the

**Fig. 4** Plots of  $\log k_N$  for the reactions of DNBSCl with piperidine in a series of COS and RTILs against  $\alpha$ .

latter, a charged probe should be used to account for the cation–anion interaction and the performance depends on the solvatochromic dyes used.<sup>25</sup> The large variations found in LSER values given by different dyes used prevent a direct comparison of results obtained with a different probe in the same analysis.<sup>25</sup>

Fig. 4 shows the relationships between  $\log k_N$  and  $\alpha$  parameter<sup>23</sup> for those reactions that proceed in COS *via* a non-catalyzed route (shown in Fig. 1) and RTILs.  $\alpha$  value of an RTIL is largely determined by the availability of HBA sites on the cation.<sup>25</sup> Here we have again two regions worth analyzing: the first corresponds to a group containing COS and RTILs which present high rate constants independent of their  $\alpha$  values. This result confirms that the polarity of the medium is a determinant in the stabilization of the intermediate thereby enhancing the reaction rate. The second group includes alcohols and EAN. Note that EAN is a unique RTIL that presents a low rate coefficient comparable with that of alcohols, a result that can again be traced to their low polarity.

Welton *et al.*<sup>30</sup> reported on the reaction of methyl *p*-nitrobenzenesulfonate with a series of amines in RTILs and found that as the hydrogen bond donor ability ( $\alpha$ ) of the RTILs is increased the nucleophilicity of the amines is evidently reduced but in our case we do not find this behavior for the nucleophilicity of piperidine, except in EAN with a high  $\alpha$  value and a low rate constant.

Fig. 5 shows the relationships between  $\log k_N$  and the  $\beta$  parameter<sup>23</sup> for COS shown in Fig. 1 and RTILs. The  $\beta$  value of an RTIL is controlled primarily by the anion, with basicity increasing as the strength of the conjugate acid of the anion decreases; and its antagonistic possibility of HBA on the cation.<sup>25</sup> Fig. 5 display similar trends to those shown in Fig. 4. Here again we have two regions grouped independent of their  $\beta$  value.

Fig. 6 shows the relationship between  $\log k_N$  and the  $\pi^*$  parameter<sup>23</sup> for COS shown in Fig. 1 and RTILs.

Welton *et al.*<sup>30</sup> found that all the RTILs they used presenting high values of  $\pi^*$ , with little variation between them, should

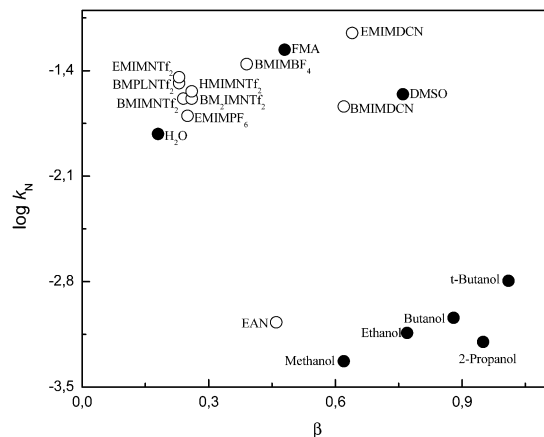


Fig. 5 Plots of  $\log k_N$  for the reactions of DNBSCl with piperidine in a series of COS and RTILs against  $\beta$ .

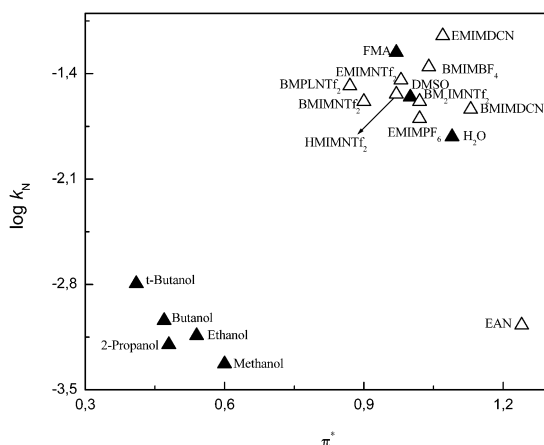


Fig. 6 Plots of  $\log k_N$  for the reactions of DNBSCl with piperidine in a series of COS and RTILs against  $\pi^*$ .

always lead to an increased rate for its and similar reactions. Apparently, in our case, this applies for all RTILs studied, except for EAN, that present a high  $\pi^*$  value and a low rate constant. Note that here again the polarity of the medium is the determinant in the stabilization of the intermediate and therefore of the reaction rate.

To close our study, we made an additional analysis performed by fixing the cation (EMIM in the present case) and varying the anionic counterpart (*i.e.* to evaluate the anion effect). Fig. 7 and 8 summarize the comparison between  $k_{\text{obs}}$  and  $[N_T]$  for the EMIM and NTF<sub>2</sub> series, respectively. Other comparisons are shown in ESI† (Fig. S68–S71).

Following a suggestion made by a reviewer, we performed a complete multiparametric correlation among our  $\log k_N$  and the hydrogen bond acidity ( $\alpha$ ), the hydrogen bond basicity ( $\beta$ ) and solvent polarity ( $\pi$ ) Kamlet–Taft (KT) solvent parameters taken from the literature. The KT analysis of solvation effects shows similar trends to that shown in Fig. 4–6 obtained from a one parameter plot. These correlations are reported in ESI† Fig. S72 and S73.

The results show the following order of decreasing quality as reaction media:  $[\text{DCN}]^- > [\text{SCN}]^- > [\text{BF}_4]^- > [\text{NTF}_2]^- > [\text{FAP}]^-$ .

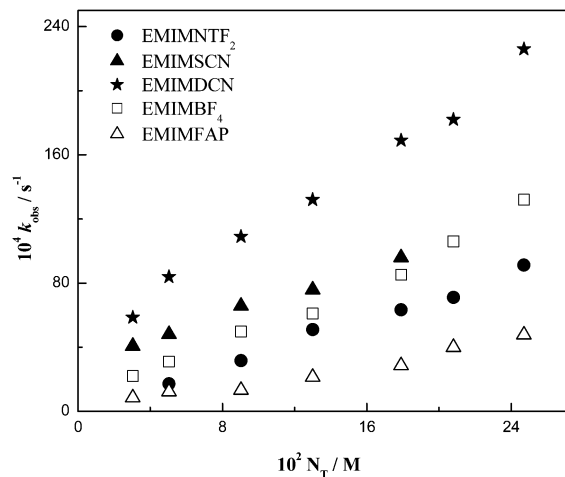


Fig. 7 Comparison between  $k_{\text{obs}}$  against total amine concentration  $[N_T]$  for the reaction of DNBSCl with piperidine in EMIMNTF<sub>2</sub>, EMIMSCN, EMIMDCN, EMIMBF<sub>4</sub> and EMIMFAP at 25.0 °C.

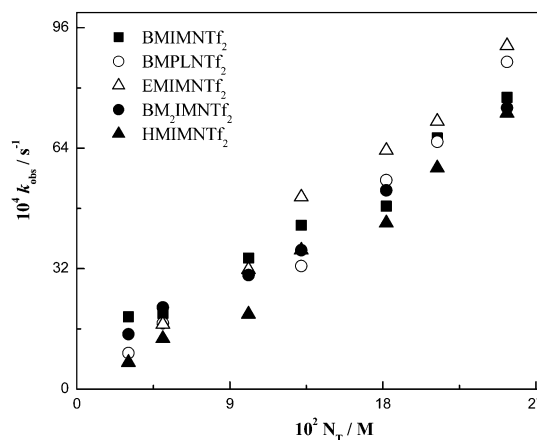


Fig. 8 Comparison between  $k_{\text{obs}}$  against total amine concentration  $[N_T]$  for the reaction of DNBSCl with piperidine in BMIMNTF<sub>2</sub>, EMIMNTF<sub>2</sub>, BMPLNTF<sub>2</sub>, BM<sub>2</sub>IMNTF<sub>2</sub> and HMIMNTF<sub>2</sub> at 25.0 °C.

This result may be attributed to the significantly high polarizability of the dicyanamide anion, which presents a highly rich  $\pi$  electron density. An additional factor seems to be the size of the anion which shows an inverse relationship with the reaction rate. Even though we do not have enough information to rationalize these results it could be related to steric hindrance effects.

We considered a similar analysis but this time fixing the anion  $[\text{NTF}_2]^-$  and varying the cation. No significant differences in reaction rates were observed by changing the length of the alkyl chain of the imidazole from two to six carbons, even if the acidic proton of the imidazole is blocked (see Fig. 8). Apparently, the steric hindrance effects going from two to six carbon atoms in the alkyl chain in the cation is less important than changes in the size of the anion.

A striking observation is that EMIMDCN and BMIMDCN only differing in the alkyl chain on the cation display quite different rate coefficients. One possibility is to have both RTILs with a significant amount of water. We proceeded then to

repeat the kinetic measurements after drying both solvents for 8 hours in a vacuum drying oven at a pressure of  $-0.06$  MPa. The same kinetic results were obtained. It seems that kinetic data are not sufficient to settle these differences which could be elucidated with the aid of theoretical studies introducing electronic structure information. Work along this line is in course in our group.

## Conclusions

Solvation effects on the reaction mechanism of the title reactions have been kinetically evaluated for a set of 21 conventional solvents and 17 RTILs. Solvent polarity affects the catalyzed and non-catalyzed  $S_NAr$  pathways differently. The competitive  $S_N$  product is not observed at the end of the reaction under pseudo first order conditions verified by HPLC analyses. The study of solvent polarity performed on the series of COS plus water and FMA reveals that HB ability drives the  $S_NAr$  process in the non-catalyzed route in Scheme 1. The role of water and FMA is the most significant due to its amphiphilic character as an HB donor and an HB acceptor that results in a nucleophilic activation at the nitrogen center of piperidine. It is relevant to note that RTILs performed relatively well in comparison with COS. The ionic liquid EMIMDCN appears to be the best solvent for this  $S_NAr$  route, a result probably due to the high polarizability of the dicyanamide anion.

## Experimental section

### Materials

Piperidine was purified before use. All the solvent used were commercially available by Sigma-Aldrich and Merck with purity  $\geq 99\%$ , stored under anhydrous conditions and used as received. The certificate of analysis given by Merck S.A. of all RTILs show purity values between 99 and 100%, presence of halides  $\leq 0.1\%$  and content of water  $\leq 1\%$ . To ensure that they had no water, we put the RTILs into a vacuum drying oven LabTech Model LVO-2013 for 4 hours at a pressure of  $-0.06$  MPa before use.

### Synthetic protocol of 1-(2,4-dinitrophenyl)piperidine

To a solution of 1-chloro-2,4-dinitrobenzene (200 mg, 0.99 mmol) in dry DMSO (2.0 mL), containing potassium carbonate (280 mg, 2.03 mmol), was added piperidine (169 mg, 1.98 mmol). The mixture was stirred for 12 h at room temperature and the reaction mixture was poured onto ice-water (20 g). The solid was filtered, washed with water, dried and recrystallized from ethanol to give 1-(2,4-dinitrophenyl)piperidine (180 mg, 73%), mp  $92-93$  °C (Lit.<sup>31</sup>  $91-92.5$  °C).  $^1H$  (400 MHz,  $CDCl_3$ ):  $\delta$  1.65–1.80 (m, 6H), 3.20–3.30 (m, 4H), 7.08 (d,  $J = 9.4$  Hz, 1H), 8.21 (dd,  $J = 9.4, 2.7$  Hz, 1H), 8.69 (d,  $J = 2.7$  Hz, 1H).

### Synthetic protocol of 1-(2,4-dinitrophenylsulfonyl)piperidine

To a solution of 2,4-dinitrobenzenesulfonyl chloride (2.67 g, 10 mmol) in dichloromethane (35 mL), piperidine (0.85 g, 10 mmol) at  $0$  °C. The mixture was stirred for 4 hours and

the reaction mixture was diluted with dichloromethane (50 mL), washed with 1 N HCl (15 mL), brine and dried. The solvent was removed under reduced pressure and the residue was purified by column chromatography on silica gel using ethyl acetate–hexane 1:5 to give 1.85 g of a white product (59%), mp  $128-130$  °C (Lit.<sup>32</sup>  $130$  °C).  $^1H$  NMR  $\delta$  1.58–1.80 (m, 2H), 1.80–1.84 (m, 4H), 3.54–3.70 (m, 4H), 8.21 (d,  $J = 8.6$  Hz, 1H), 8.45 (d,  $J = 2.0$  Hz, 1H), 8.49 (dd,  $J = 2.0, 8.6$  Hz, 1H).

### Kinetic measurements

The kinetics of the reactions were measured using a diode array spectrophotometer in water at  $25.0$  °C and an ionic strength of  $0.2$  M (maintained with KCl), by monitoring (380 nm) the formation of product 3. The kinetic measurements in COS, RTILs and 90/10 ethanol/water mixture were made in the absence of KCl and at 350–400 nm at the same temperature. The initial substrate concentration was  $5 \times 10^{-5}$  M. Under excess amine, pseudo-first-order rate coefficients ( $k_{obs}$ ) were found throughout. For the reactions *via* non-catalyzed the  $k_{obs}$  values were obtained through the kinetic software (for first-order reactions) of the spectrophotometer. For the reactions occurring *via* catalyzed pathways, the validation that the reaction proceeds as shown in Scheme 1 is done through the observation that the plots of  $k_{obs}/[N_T]$  vs.  $[N_T]$  are linear.  $Kk_2$  values are obtained from the intercept of these graphs and  $Kk_3$  is obtained from the slope of these graphs.

### Chromatographic system and conditions

The HPLC system used for the analysis of the samples was a UV-DAD Elite Lachrom equipped with a quaternary pump L-2100 with a UV-DAD detector L-2455, an 8  $\mu$ L injection loop, an oven column L-2300 and an autosampler L-2200 with a cooling unit. The column attached was a Chromolith Fast Gradient RP 18 50–3 mm (Merck). The UV detector was set at 260 nm which was found to be the most suitable wavelength for the detection of all the substrates, product and internal standard. The flow-rate of the mobile phase was adjusted to  $0.5$  mL  $min^{-1}$  to keep the column pressure between 47–50 bar. The system was thermostated at  $25$  °C to maintain the same reactions conditions. Chromatograms were recorded in a computer system using EZChrom Elite software from Agilent.

## Acknowledgements

This work was supported by Project ICM-P10-003-F CILIS, granted by Fondo de Innovación para la Competitividad del Ministerio de Economía, Fomento y Turismo, Chile; Fondecyt grants 1100492 and 1110062. M.G. acknowledges support from Conicyt under the postdoctoral fellowship 3120060.

## Notes and references

- 1 J. F. Bunnett and R. E. Zahler, *Chem. Rev.*, 1951, **49**, 273; J.-H. Choi, B.-C. Lee, H.-W. Lee and I. Lee, *J. Org. Chem.*, 2002, **67**, 1277; I.-H. Um, J.-Y. Hong, J.-J. Kim, O.-M. Chae

- and S.-K. Bae, *J. Org. Chem.*, 2003, **68**, 5180; I.-H. Um, S.-M. Chun, O.-M. Chae, M. Fujio and Y. Tsuno, *J. Org. Chem.*, 2004, **69**, 3166; I.-H. Um, J.-Y. Hong and J.-A. Seok, *J. Org. Chem.*, 2005, **70**, 1438.
- 2 A. Williams, *Concerted Organic and Bio-organic Mechanisms*, CRC Press, Boca Raton, FL, 2000, ch. 4, p. 43.
  - 3 O. Banjoko and I. A. Babatunde, *Tetrahedron*, 2004, **60**, 4645.
  - 4 R. Ormazabal-Toledo, J. G. Santos, P. Ríos, E. A. Castro, P. R. Campodónico and R. Contreras, *J. Phys. Chem. B*, 2013, **117**, 5908.
  - 5 R. Ormazabal-Toledo, R. Contreras, R. A. Tapia and P. R. Campodónico, *Org. Biomol. Chem.*, 2013, **11**, 2302.
  - 6 R. Ormazabal-Toledo, R. Contreras and P. R. Campodónico, *J. Org. Chem.*, 2013, **78**, 1091.
  - 7 C. F. Bernasconi, *MTP Int. Rev. Sci.: Org. Chem., Ser. One*, 1973, **3**, 33.
  - 8 I.-H. Um, S.-W. Min and J.-M. Dust, *J. Org. Chem.*, 2007, **72**, 8797.
  - 9 N. S. Nudelman, P. M. E. Mancini, R. D. Martínez and L. R. Vottero, *J. Chem. Soc., Perkin Trans. 2*, 1987, 951.
  - 10 X. L. Wang, E. J. Salaski, D. M. Berger and D. Power, *Org. Lett.*, 2009, **11**, 5662.
  - 11 S. Park and S. Lee, *Bull. Korean Chem. Soc.*, 2010, **31**, 2571.
  - 12 I. Newington, J. M. Perez-Arlandis and T. Welton, *Org. Lett.*, 2007, **9**, 5247.
  - 13 F. D'Anna, S. Marullo and R. Noto, *J. Org. Chem.*, 2010, **75**, 767.
  - 14 F. D'Anna, V. Frenna, R. Noto, V. Pace and D. Spinelli, *J. Org. Chem.*, 2006, **71**, 5144.
  - 15 F. D'Anna, S. Marullo and R. Noto, *J. Org. Chem.*, 2008, **73**, 6224.
  - 16 C. C. Weber, A. F. Masters and T. Maschmeyer, *Org. Biomol. Chem.*, 2013, **11**, 2334.
  - 17 C. A. Angell, N. Byrne and J.-P. Belieres, *Acc. Chem. Res.*, 2007, **40**, 1228.
  - 18 E. Buncl, J. M. Dust and F. Terrier, *Chem. Rev.*, 1995, **95**, 2261.
  - 19 M. R. Cramptom, *Adv. Phys. Org. Chem.*, 1969, **7**, 211.
  - 20 W. P. Jencks, *Chem. Rev.*, 1985, **85**, 511; E. A. Castro, *Chem. Rev.*, 1999, **99**, 3505.
  - 21 E. A. Castro, M. Aliaga, M. Gazitúa and J. G. Santos, *Tetrahedron*, 2006, **62**, 4863.
  - 22 F. G. Bordwell and D. L. Hughes, *J. Am. Chem. Soc.*, 1986, **108**, 5991.
  - 23 M. J. Kamlet, J. L. M. Abboud, M. H. Abraham and R. W. Taft, *J. Org. Chem.*, 1983, **48**, 2877.
  - 24 A. Cerda-Monje, A. Aizman, R. A. Tapia, C. Chiappe and R. Contreras, *Phys. Chem. Chem. Phys.*, 2012, **14**, 10041.
  - 25 J. P. Hallett and T. Welton, *Chem. Rev.*, 2011, **111**, 3508.
  - 26 R. Bini, C. Chiappe, V. L. Mestre, C. S. Pomelli and T. Welton, *Org. Biomol. Chem.*, 2008, **6**, 2522.
  - 27 P. G. Jossop, D. A. Jossop, D. Fu and L. Phan, *Green Chem.*, 2012, **14**, 1245.
  - 28 M. A. Ab-Rani, A. Brant, L. Crowhurst, A. Dolan, M. Lui, N. H. Hassan, J. P. Hallett, P. A. Hunt, H. Niedermeyer, J. M. Perez-Arlandis, M. Shrems, T. Welton and R. Wilding, *Phys. Chem. Chem. Phys.*, 2011, **13**, 16831.
  - 29 A. C. Kenneth, *Chemical Kinetics: The study of reaction rates in solution*, John Wiley & Sons, New York, USA, 1990, p. 236.
  - 30 L. Crowhurst, L. Lancaster, J.-M. Pérez-Arlándiz and T. Welton, *J. Am. Chem. Soc.*, 2004, **126**, 11549.
  - 31 J. F. Bunnett and G. T. Davis, *J. Org. Chem.*, 1954, **76**, 3011.
  - 32 J. D. Loudon and N. Shulman, *J. Chem. Soc.*, 1938, 1926.